Proceedings of the 5th International Symposium on Steel Science (ISSS 2017)
Nov. 13-16, 2017, Kyoto, Japan: The Iron and Steel Institute of Japan

Influence of grain boundary segregation on temper embrittlement of Cr-Mo heat resistant steel weld metal and quantitative analysis of the amount of segregated atoms

Hidenori Nako[1*], Genichi Taniguchi[2], Su-Qin Zhu[3], Simon P. Ringer[3]

[1] Materials Research Laboratory, Kobe Steel, Ltd., 1-5-5 Takatsukadai Nishi-ku, Kobe, Hyogo, Japan
[2] Welding Business, Kobe Steel, Ltd., 100-1 Miyamae, Fujisawa, Kanagawa, Japan
[3] The University of Sydney, Faculty of Engineering and Information Technologies, School of Aerospace, Mechanical and Mechatronic Engineering, Australian Centre for Microscopy & Microanalysis, The University of Sydney, NSW 2006, Australia

Abstract: Influence of P segregation on temper embrittlement has been investigated using three dimensional Atom Probe Tomography (APT). VC and M_7C_3 are observed at a Prior-Austenite Grain Boundary (PAGB) of 2.25Cr-1Mo-V steel weld metal by APT analysis. P atoms are detected within a VC particle at PAGB and at M_7C_3/matrix interface, and not observed at VC/matrix interface. The weld metal containing larger amount of VC shows higher temper embrittlement resistance. It is considered that VC formed at PAGB inhibits temper embrittlement by decreasing the area of P-segregated PAGB. The formation of M_7C_3 at PAGB also decreases P-segregated PAGB. However, it is probable that the strength of M_7C_3/matrix boundary lowers due to the P segregation, resulting in less effective to improve the temper embrittlement.

Additionally, the Interfacial Excess (IE) of P atoms at grain boundaries with various character, i.e. Σ3 coincidence boundary, high and low angle random boundaries, have been compared in Fe-Mn-P (Base) and Fe-Mn-P-Cr (Cr-added) alloys. IE of P shows a good relationship with the grain boundary energy. Moreover, the IE in the Cr-added alloy is higher than in the base alloy. This implies that Cr addition has a negative effect on the temper embrittlement by promoting P segregation.

1. INTRODUCTION

It is known that phosphorous (P) degrades mechanical properties of iron alloys. A typical example is the temper embrittlement. P atoms segregate at Prior-Austenite Grain Boundary (PAGB) during temper treatment, resulting in promotion of grain boundary fracture and lowering of toughness [1-5]. Hence, it is essential to inhibit the temper embrittlement for tempered or heat resistant steels, i. e. Cr-Mo steel used for the reactors for oil refineries.

Temper embrittlement is promoted in alloy steels containing Mn, Cr and Ni [6]. Many authors have been examined the effect of alloy elements on P segregation and temper embrittlement. Yu et al investigated the influences of Si and Mn on P segregation using Auger Electron Spectroscopy (AES) and revealed that both Si and Mn promote P segregation. They concluded that Si raise the activity of P, resulting in the increase in P segregation. On the other hand, it is considered that the promotion of P segregation by Mn addition is due to the co-segregation of Mn and P [5]. Grabke et al reported that solute Ti and Nb inhibit P segregation [7]. Some studies have pointed out that C has a repulsive interaction with P and decreases the amount of segregated P atom [7, 8]. Mo has been regarded as a favourable element to suppress P segregation by forming Mo-P cluster [5]. From the viewpoint of carbide precipitation, it is reported that TiC particles retain P within ferrite grain and hence decrease P segregation [7]. Mo_2C act as trapping sites of P [7]. Inoue et al compared Fe-C-P alloy and 2.25Cr-1Mo steel and presumed that grain boundary carbide causes degradation of temper embrittlement resistance. However, effect of carbide formation at PAGB on P segregation and temper embrittlement still remain to be clarified. In the present study, influences of carbide formation and P segregation at boundaries on temper embrittlement are investigated using three dimensional Atom Probe Tomography (APT). In addition, relationship between grain boundary character and the amount of segregated P atom detected by APT is examined.

* Corresponding author. E-mail: nako.hidenori@kobelco.com, telephone: +81 78 992 5503.

2. EXPERIMENTAL

Three multi-pass weld metals were deposited in 20-degree V-grooves with a 19mm root gap by shield metal arc welding process. The welding current, voltage, speed, and preheat/interpass temperature were 215 A, 26 V, approximately 2 mm/s and 200-220 °C, respectively. Base, V-added and Cr-added weld metals were prepared to vary the amount of carbides. Table 1 shows the chemical compositions of the weld metals. The weld metals were heated at 705 °C as post-weld heat treatment (PWHT). Subsequently, the step cooling (SC) treatment was conducted to promote temper embrittlement [9]. Toughness of the weld metals was measured using the transition temperature with the absorption energy of 54 J (vTr_{54}) both at as-PWHT and PWHT+SC conditions. Temper embrittlement was evaluated using a change in vTr_{54} by the SC process. Charpy specimens vertical to the welding direction were cut from the centre of thickness position in the weld metals. The notch position was located at the centre of the weld metal.

Observations of microstructure, carbides, P segregation were carried out at the as-welded zone (final-pass) of the weld metals since the centre of the weld metal, where notch was located, showed complicated microstructure because of the multiple thermal cycles. Microstructures were observed with light optical microscopy (OM). The cross-sections of the weld metals normal to the welding direction were polished and etched with 3% nital solution (3% nitric acid and 97% methanol) before observation. Selected area electron diffraction (SAED) pattern and energy dispersive X-ray spectroscopy (EDS) by transmission electron microscopy (TEM) analyses were made for identifying the carbides at PAGBs. Specimens for TEM analysis were made by replica technique. Concentrations of insoluble elements in the weld metals were measured by electrolytic extraction residue technique to estimate the amounts of various carbides. APT analysis was conducted in a volume containing a PAGB. Specimens for APT analysis were prepared using focused ion beam. APT measurements were carried out on a voltage pulsed atom probe equipped with a large angle reflectron, CAMECA LEAP 3000HR™ at a specimen temperature of -223 °C and a pulse fraction of 25-30 %.

Table 1 Chemical composition of the weld metals (mass %)

	C	Si	Mn	P	Cr	Mo	V	Nb	Fe	X-bar*	J-Factor**
Base	0.084	0.32	1.00	0.006	2.39	1.05	0.32	0.022	bal.	8.8	132
V-added	0.087	0.28	0.95	0.006	2.41	1.05	0.37	0.021	bal.	8.2	123
Cr-added	0.086	0.27	0.96	0.006	2.65	1.05	0.29	0.018	bal.	8.2	123

*X-bar = (10P+5Sb+4Sn+As)/100 (mass ppm)
**J-Factor =(Si+Mn)(P+Sn)×10^4 (mass %)

3. RESULTS

3.1. Temper embrittlement

vTr_{54} values of the weld metals are shown in Fig. 1. The vTr_{54} values of the weld metals become higher by the SC process due to the temper embrittlement. Change in vTr_{54} of V-added weld metal is smaller than that of Base specimen. This indicates V addition inhibit the temper embrittlement. Cr-added weld metal show higher vTr_{54} than Base specimen both at As-PWHT and PWHT+SC conditions. Cr addition has little effect on temper embrittlement resistance.

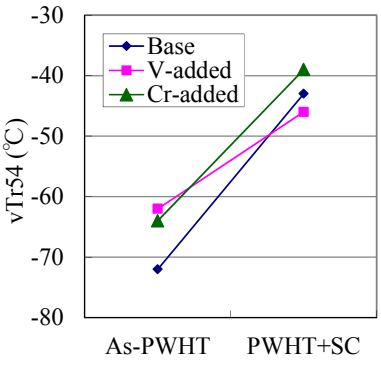

Fig. 1 vTr_{54} of the weld metals.

3.2. Microstructure and carbides precipitation

Fig. 2 shows the optical micrographs of the weld metals after PWHT+SC process. Martensitic microstructures are formed and PAGBs are clearly observed in all the weld metals. Grain boundary ferrite is not found in any of the weld metals.

Fig. 3 shows TEM image, SAED pattern, and EDS histogram of carbides formed at PAGB in the Base weld metal after PWHT. $M_{23}C_6$, M_7C_3 and MC are observed. $M_{23}C_6$ and M_7C_3 contain Cr, Mo and Fe. MC is composed of mainly V. The amounts of insoluble V, Mo, Cr, and Fe in the weld metals after PWHT+SC process are shown in Fig. 4. V addition increases the amount of insoluble V. Considering the result of TEM analysis, it is supposed that the concentration of insoluble V is related

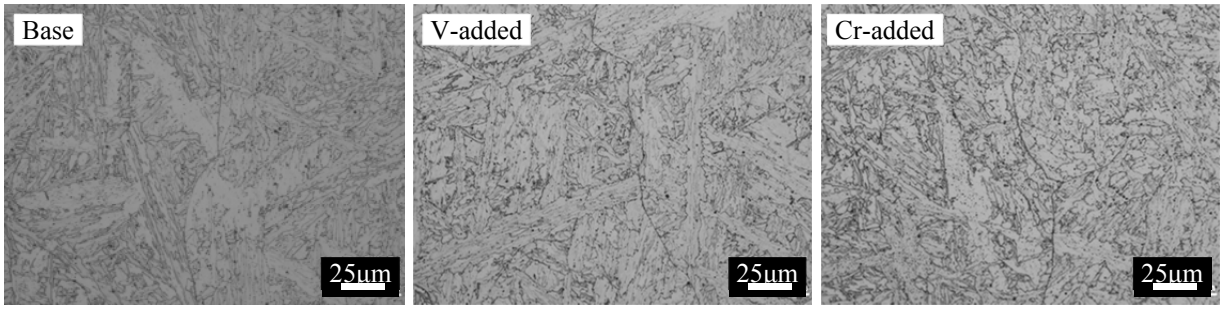

Fig. 2 Optical micrographs of the weld metals after PWHT+SC process.

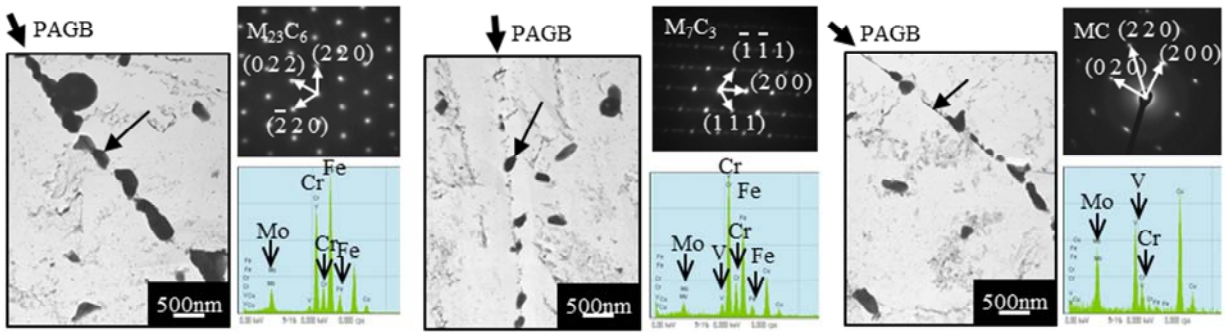

Fig. 3 Replica TEM images, SAED patterns, and EDS histograms of carbides formed at PAGB in the Base weld metal after PWHT. SAED patterns and EDS histograms are obtained from the arrowed carbide [10].

to the amount of VC. Also, the concentrations of insoluble Cr and Fe are considered to correlate with the amounts of $M_{23}C_6$ and M_7C_3. Thus, it is concluded that the V addition increased the amount of VC and decreased the amounts of $M_{23}C_6$ and M_7C_3.

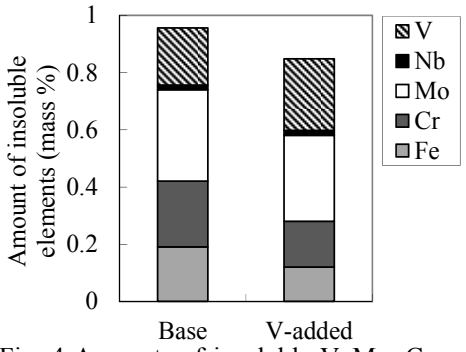

Fig. 4 Amounts of insoluble V, Mo, Cr, and Fe in the weld metals after PWHT+SC process.

3.3. APT analysis

Fig. 5 shows P atom map of the Base weld metal. Segregation of P atoms is detected along the PAGB both at as-PWHT and PWHT+SC conditions. Apparently, the number of P atoms segregated at PAGB becomes larger after the SC process. It is considered that the increase in P segregation causes the temper embrittlement as referred in previous studies [1-5]. It is considered that the temper embrittlement is mainly caused by the P segregation at PAGB in the present study. Fig. 6 displays atom maps of the analysis volume containing a PAGB and grain boundary carbides in the Base weld metal. The region A where C, Cr and V atoms are highly concentrated is identified as M_7C_3 since the Cr/Mo ratio within the region A (approximately 10) is close to the Cr/Mo ratio in M_7C_3 phase calculated using Thermo-Calc® software (8.6). The region B, in which C and V atoms are enriched, is VC. Fig. 7 shows P, Cr and V concentration profiles across (a) VC and (b) M_7C_3 in the analysis volume shown in Fig. 6. P atoms are detected within the VC particle. In addition, P segregation at the interface between M_7C_3 and the matrix is observed.

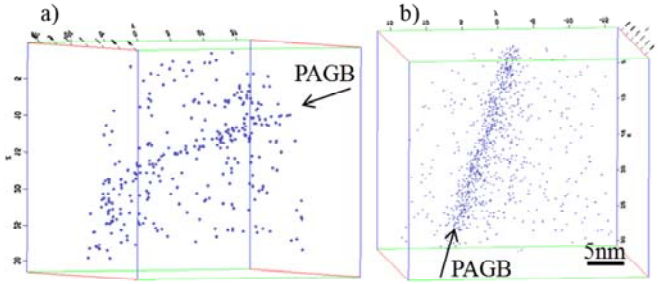

Fig. 5 P atom maps of the Base weld metal after a) PWHT and b) PWHT+SC process.

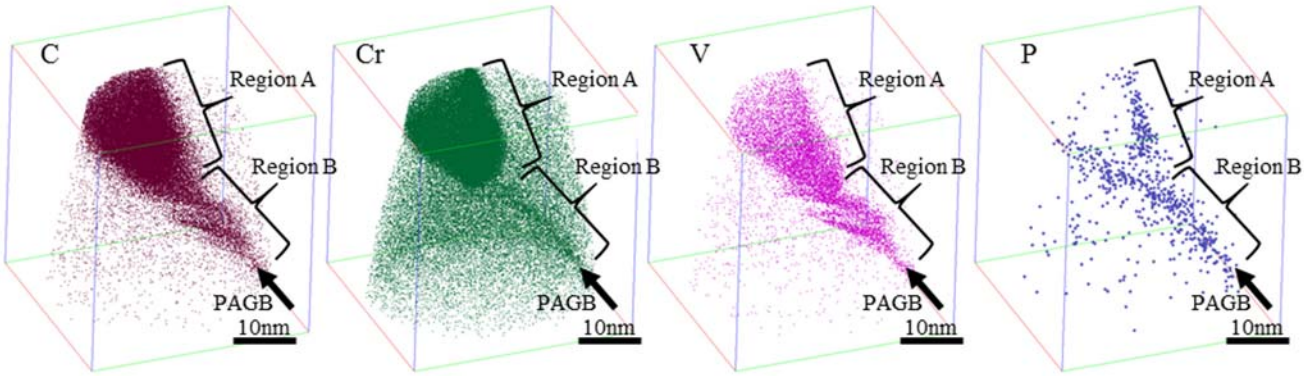

Fig. 6 C, Cr, V, and P atom maps of the Base weld metal after PWHT [10].

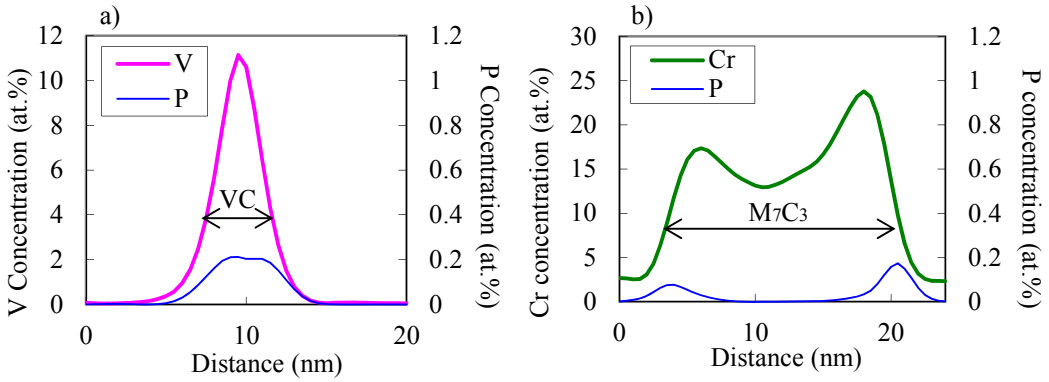

Fig. 7 P, Cr, and V concentration profiles across (a) VC and (b) M_7C_3 in the volume displayed in Fig. 6 [10].

4. DISCUSSION

The V-added weld metal shows the higher temper embrittlement resistance than the Base weld metal. Fig. 8 shows the interfacial excess (IE) of P atoms at PAGB in the Base and V-added weld metals. It seems that the average IE of the V-added weld metal is larger than that of the Base weld metal though it should be noted that the deviations of IE value are large. This implies that the higher temper embrittlement resistance of the V-added weld metal is not explained from the viewpoint of the number of P atoms per unit area of PAGB.

As for the carbides, V addition increases the amount of VC, which is finer than $M_{23}C_6$ or M_7C_3, and reduces the amounts of $M_{23}C_6$ and M_7C_3. It is probable that the decrease of the amount of coarse $M_{23}C_6$ or M_7C_3 particles has a favourable effect on the toughness of the weld metals [11]. However, the toughness of the V-added weld metal is inferior to the Base weld metal at the as-PWHT condition. This implies that the influence of the carbide size on the toughness is small in the present study.

It would be worth noting that P atoms were detected within VC particles at PAGB and not observed at VC/matrix interface. Assuming that the strength of VC/matrix interface without P segregation is higher than P-segregated PAGB, the formation of VC at PAGB may improve the temper embrittlement resistance by decreasing the area of P-segregated PAGB. Thus, it is considered that the improvement of temper embrittlement resistance in the V-added weld metal is derived from the increase of VC particles at PAGB. It is expected that the formation of M_7C_3 at PAGB may have a positive effect on the temper embrittlement resistance since M_7C_3 also reduce the area of P-segregated PAGB. However, the temper embrittlement resistance of the Cr-added weld metal, which contains more M_7C_3, is not improved compared to the Base weld metal. To explain the temper embrittlement in the Cr-added weld metal, P segregation at

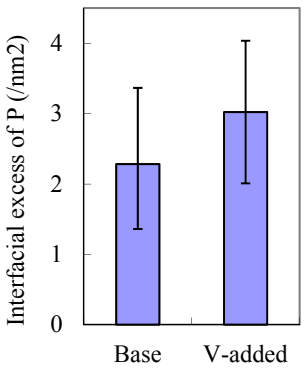

Fig. 8 IE of P at PAGBs in the Base and V-added weld metals after PWHT+SC process.

carbide/matrix interface should be considered. P atoms are detected at the M_7C_3/matrix interface in this study, unlike the VC/matrix interface. Hence, M_7C_3 formation at PAGB results in not only the decrease in the area of P-segregated PAGB but also the increase in the area of P-segregated M_7C_3/matrix interface. In case that the P segregation may decrease the strength of M_7C_3/matrix interface, it is supposed that the temper embrittlement resistance of the Cr-added weld metal is derived from the combination of positive (decrease in P-segregated PAGB) and negative (increase in P-segregated M_7C_3/matrix interface) effects.

5. INFLUENCE OF GRAIN BOUNDARY CHARACTER ON THE AMOUNT OF P SEGREGATION

As displayed in Fig. 8, the IE values of P at PAGB in the Base and V-added weld metals contain large deviation. As for the V-added weld metal, maximum IE value is twice as large as the minimum. It is supposed that the deviation is mainly caused by the difference of grain boundary character [12]. Then, the influence of grain boundary character on the IE of P is investigated using Fe alloys. The chemical compositions of the alloys are shown in Table 2.

Table 2 Chemical compositions of the Fe-alloys (mass %)

	Mn	P	Cr	Fe
Base	1.45	0.013	<0.02	bal.
Cr-added	1.44	0.013	2.20	bal.

The alloys were prepared by arc melting. Bar specimens (12mmΦx100mmL) were obtained by forging following the heat treatment at 1300 °C for 2 hours. Subsequently, the specimens were held at 1000 °C for 1 hour and water-quenched followed by the SC process. A low angle grain boundary (LAGB) with the rotation angle of less than 10°, two random high angle grain boundaries (HAGBs) with the rotation angle of approximately 30° and 50°, and $\Sigma3_{<111>60°}$ grain boundary (Σ3 GB) were selected using EBSD. Specimens containing various grain boundaries were analysed using APT (LEAP3000XSi or LEAP4000XSi with voltage pulse mode) at -253~-233 °C.

P atom maps of the Cr-added alloy are depicted in Fig. 9. P atoms are detected along LAGB, HAGBs and Σ3 GB. Fig. 10 shows the relationship between Cr content and IE of P atoms in the Fe-alloys after the SC process. Cr addition promotes P segregation at 30° HAGB. This implies that Cr addition has a negative effect on the temper embrittlement by promoting P segregation. In contrast, the influence of Cr addition on P segregation at Σ3 GB is small. Fig. 11 shows IEs

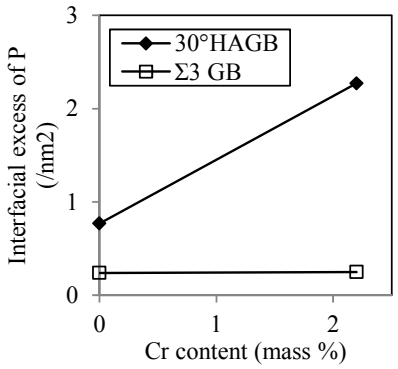

Fig. 10 Relationship between Cr content and IE of P at grain boundary in the Fe-alloys after the SC process.

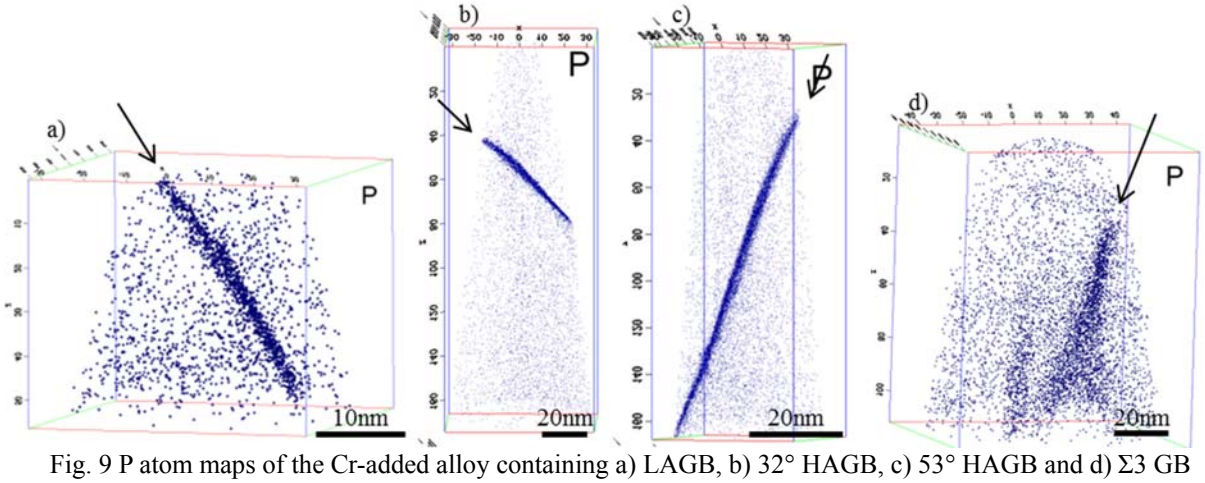

Fig. 9 P atom maps of the Cr-added alloy containing a) LAGB, b) 32° HAGB, c) 53° HAGB and d) Σ3 GB after the SC process. Allows indicate the grain boundaries.

of P at various grain boundaries in the Cr-added alloy. IEs of P at HAGBs show approximately 2 /nm^2 regardless the difference of rotation angle. IEs at LAGB and Σ3 GB are much less than that of HAGBs.

It is known that segregation at grain boundary is influenced by the grain boundary energy. Thus, IE is evaluated from the viewpoint of grain boundary energy. In Shibuta's study, energies of symmetric tilt boundaries of iron have been calculated by molecular dynamics [13]. Based on his result, energies of LAGB, 30 and 50° HAGBs, and Σ3 GB are estimated as 0.4, 1.5, 1.5 and 0.5 J/m^2 respectively though it should be noted that the grain boundaries in the present study are not tilt boundaries. IE of P and estimated grain boundary energy are plotted in Fig. 12. Positive correlation between IE of P and the grain boundary energy is obtained. Uesugi and Higashi have revealed that the grain boundary free excess volume, which is defined as the increment of free volume per unit area of grain boundary by introduction of grain boundary, increases linearly as grain boundary energy increases using the first-principal calculation in pure-Al [14]. It is considered that a grain boundary with low energy, such as LAGB or coincidence boundary, does not allow a larger amount of P segregation due to the small free excess volume. On the contrary, IE of P becomes larger at a random HAGB with a larger free excess volume. IEs of P at random HAGBs show approximately the same value despite the difference of rogation angles as shown in Fig. 11. It is supposed that this result is because the difference of grain boundary energy, that is, free excess volume is small among random HAGBs.

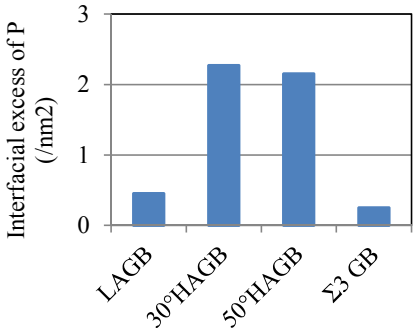

Fig. 11 IE of P at various grain boundaries in the Cr-added alloy after the SC process.

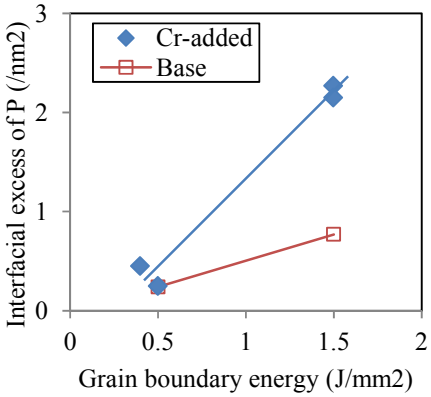

Fig. 12 Relationship between estimated grain boundary energy and IE of P at grain boundary in the Base and Cr-added alloys after the SC process.

6. CONCLUSION

The influence of P segregation on temper embrittlement is studied in Cr-Mo steel weld metals. V addition increases the amount of VC and improves temper embrittlement resistance since VC formed at PAGB reduces the area of P-segregated PAGB which causes the temper embrittlement. M_7C_3 also decreases the area of P-segregated PAGB. However, P atoms segregate at M_7C_3/matrix interface, which may lower the strength of M_7C_3/matrix interface. As a result, Cr addition is not effective to inhibit temper embrittlement. Interfacial excess value of P atom at grain boundary contains a large deviation, which is derived from the difference of grain boundary energy.

REFERENCES

[1] M. Nakamura, T. Shinoda, H. Watanabe: Tetsu-to-Hagané, 65 (1979), 1926-1935.
[2] T. Inoue, K. Yamamoto: Tetsu-to-Hagané, 69 (1979), A105-A108.
[3] H. Nakata, K. Fujii, K. Fukuya, M. Shibata, R. Kasada, A. Kimura: INSS Journal, 9 (2002), 171-176.
[4] J. Yu, C. J. MacMahon, Jr: Metall. Trans. A, 11A (1980), 277-289.
[5] J. Yu, C. J. MacMahon, Jr: Metall. Trans. A, 11A (1980), 291-300.
[6] J. Hollomon: Trans. ASM, 36 (1946), 473-542.
[7] H. J. Grabke, R. Möller, H. Erhart, S. S. Brenner: Surface and Interface Analysis, 10 (1987), 202-209.
[8] H. J. Sung, N. H. Heo, S-J. Kim: Metall. Mater. Trans. A, 48A (2017), 1459-1465.
[9] J. Grosse-Wördemann, S. Dittrich: Weld. J., May (1983), 123s-128s.
[10] H. Nako, Y. Okazaki, H. Hatano, G. Taniguchi, M. Otsu, K. Yamashita: Proc. ISSS 2014 (2014), 124-127.
[11] N. J. Petch: Acta Metall. 34 (1986), 1387-1393.
[12] T. Watanabe, T. Murakami, S. Karashima: Scripta Metall., 12 (1978), 361-365.
[13] Y. Shibuta, S. Takamoto, T. Suzuki: ISIJ Int., 48 (2008), 1582-1591.
[14] T. Uesugi, K. Higashi: J. Mater. Sci., 46 (2011), 4199-4205.